# Impaired mitochondrial oxidative phosphorylation in the peroxisomal disease X-linked adrenoleukodystrophy

**J. López-Erauskin[1,2,3], J. Galino[1,2,3], M. Ruiz[1,2,3], J.M. Cuezva[3,4], I. Fabregat[5], D. Cacabelos[6], J. Boada[6], J.Martínez[1,2,3], I.Ferrer[2,7], R. Pamplona[6], F. Villarroya[8,9], M. Portero-Otín[6], S. Fourcade[1,2,3], A. Pujol[1,2,3,10,*]**

[1]Neurometabolic Diseases Laboratory, Institut d'Investigació Biomèdica de Bellvitge (IDIBELL), Hospitalet de Llobregat, Barcelona, Catalonia, Spain

[2]Institut de Neuropatologia de Bellvitge, Universitat de Barcelona, L'Hospitalet de Llobregat, Barcelona, Spain

[3]Center for Biomedical Research on Rare Diseases (CIBERER), ISCIII, Spain

[4]Departamento de Biología Molecular, Centro de Biología Molecular Severo Ochoa, Consejo Superior de Investigaciones Científicas-Universidad Autónoma de Madrid (CSIC-UAM), Instituto de Investigación Hospital 12 de Octubre, Universidad Autónoma de Madrid, Madrid, Spain

[5]Biological Clues of the Invasive and Metastatic Phenotype Group, Institut d'Investigació Biomèdica de Bellvitge (IDIBELL), Hospitalet de Llobregat, Barcelona, Catalonia, Spain

[6]Departament de Medicina Experimental, Universitat de Lleida-IRB-LLEIDA, Lleida, Catalonia, Spain

[7]Center for Biomedical Research on Neurodegenerative Diseases (CIBERNED), Spain

[8]Departament de Bioquimica i Biologia Molecular and Institut de Biomedicina IBUB, Universitat de Barcelona, Barcelona, Catalonia, Spain

[9]Center for Biomedical Research on Fisiopatologia de la Obesidad y Nutrición, ISCIII, Spain

[10]Catalan Institution for Research and Advanced Studies (ICREA), Barcelona, Catalonia, Spain

[*]Correspondence should be addressed to: Aurora Pujol, Neurometabolic Diseases Laboratory, IDIBELL, Hospital Duran i Reynals, Gran Via 199, 08908 L'Hospitalet de Llobregat, Barcelona, Catalonia, Spain. Tel: +34 932607343; Fax: +34 932607414; Email: apujol@idibell.cat

**ABSTRACT**

X-linked adrenoleukodystrophy (X-ALD) is an inherited metabolic disorder of the nervous system characterized by axonopathy in spinal cords and/or cerebral demyelination, adrenal insufficiency and accumulation of very long-chain fatty acids (VLCFA) in plasma and tissues. The disease is caused by malfunction of the ABCD1 gene, which encodes a peroxisomal transporter of VLCFA or VLCFA-CoA. In the mouse, ABCD1 loss causes late onset axonal degeneration in the spinal cord, associated with locomotor disability resembling the most common phenotype in patients, adrenomyeloneuropathy. We have formerly shown that an excess of the VLCFA C26:0 induces oxidative damage, which underlies the axonal degeneration exhibited by the *Abcd1*$^{-}$ mice. In the present study, we sought to investigate the noxious effects of C26:0 on mitochondria function. Our data indicate that in X-ALD patients' fibroblasts, excess of C26:0 generates mtDNA oxidation and specifically impairs oxidative phosphorylation triggering mitochondrial ROS production from electron transport chain complexes. This correlates with impaired Complex V phosphorylative activity, as visualized by high-resolution respirometry on spinal cord slices of *Abcd1*$^{-}$ mice. Further, we identified a marked oxidation of key OXPHOS system subunits in *Abcd1*$^{-}$ mouse spinal cords at presymptomatic stages. Altogether, our results illustrate some of the mechanistic intricacies by which the excess of a fatty acid targeted to peroxisomes, activates a deleterious process of oxidative damage to mitochondria, leading to a multifaceted dysfunction of this organelle. These findings may be of relevance for patient management while unveiling novel therapeutic targets for X-ALD.

**Keywords:** X-linked adrenoleukodystrophy, mitochondrial respiration; axonal degeneration; oxidative stress; very long-chain fatty acids

## INTRODUCTION

X-linked adrenoleukodystrophy (X-ALD: McKusick no. 300100) is a rare neurodegenerative disorder characterised by an inflammatory cerebral demyelination, or a progressive axonopathy in the spinal cord, causing spastic paraparesis (1-3). With a minimum incidence of 1 in 17,000 males, X-ALD is the most frequent inherited leukodystrophy and peroxisomal disorder. It is caused by mutations in the ABCD1 gene, which encodes for an ATP-binding cassette transporter located in the peroxisomal membrane. The function of the ABCD1 protein is key in the import of very long-chain fatty acids (VLCFA, C≥22:0) and VLCFA-CoA esters into the peroxisome for degradation (4, 5). As a consequence, the loss of the ABCD1 transporter results in the accumulation of VLCFA in most patients' organs, fibroblasts and plasma due to a lack of substrate for the VLCFA β-oxidation in peroxisomes (6-8). The main accumulated VLCFA is the hexacosanoic acid, or C26:0 that serves as a pathognomonic biomarker for the biochemical diagnosis of the disease.

The classical inactivation of the ABCD1 transporter in the mouse elicits a late-onset neurodegenerative phenotype with axonal damage in the spinal cord. The inflammatory demyelination is absent in the brain of this mouse model, which rather resembles the most frequent X-ALD phenotype, the adult adrenomyeloneuropathy or AMN (9, 10). Signs of oxidative stress have been found in X-ALD patients' blood samples and post-mortem brains (11-13). In this regard, we have formerly delivered evidences for an early, at presymptomatic stages occurring oxidative stress, concomitant with a bioenergetic dysfunction characterized by depleted ATP and NADH levels (14-16). Indeed, a treatment with a mixture of antioxidants reverses oxidative damage, metabolic failure and axonal degeneration in this model, providing proof of concept on the pivotal contribution of oxidative damage to disease pathogenesis (17-19).

The combination of a disturbance in energy homeostasis with oxidative stress, involving the mitochondria as a major player, is a common phenomenon in the physiopathogenesis of age-related neurodegenerative diseases, such as Parkinson's disease (PD), Huntington's disease (HD), Alzheimer's disease (AD) or amyotrophic lateral sclerosis (20, 21). Of note, we and others have previously described ultrastructural abnormalities in mitochondria from neurons of *Abcd1*$^{-}$ and *Abcd2*$^{-/-}$ mouse spinal cords (22) and *Abcd1*$^{-}$ adrenocortical cells (23), consistent with observations in AMN patients (24, 25), and peroxisomal-deficient Zellweger patients (26) and *Pex5*$^{-/-}$ mice (27).

In the present study, we set out to investigate mitochondrial function in the most common peroxisomal disease. We reveal a defective activity of oxidative phosphorylation (OXPHOS) in fibroblasts of X-ALD patients and in spinal cord of *Abcd1*$^{-}$ mice at presymptomatic stages, using high-resolution respirometry. This is accompanied by the oxidation of the catalytic subunits of the mitochondrial Complex V/$H^{+}$-ATP synthase, a bottleneck of oxidative phosphorylation. Furthermore, taking advantage of the cellular model provided by patients' fibroblasts, we show that excess of C26:0 specifically impairs oxidative phosphorylation and generates mitochondrial ROS at complex I and II of the electron transport chain (ETC) in these X-ALD cells.

## RESULTS

### Increased oxidation of mitochondrial proteins in spinal cords of *Abcd1*$^{-}$ mice

Based on a functional genomics analysis, we recently reported several altered mitochondrial pathways, including energetic metabolism, in 12-month-old *Abcd1*$^{-}$ spinal cords (28). Also, we described oxidative lesions in proteins of *Abcd1*$^{-}$ spinal cords, and identified specific oxidation targets, including several proteins involved in

glycolysis and the tricarboxylic acid (TCA) cycle. This was accompanied by decreased levels of ATP and NADH, and several metabolites of TCA cycle (18). Most recently, we uncovered oxidation of a mitochondrial permeability transition component, the cyclophilin D (15). These experiments were performed using homogenates of whole spinal cord tissue. Because of the intrinsic limitations of 2D proteomic experiments, including the difficulty of detecting proteins in low abundance, we thought of repeating the 2D experiments on mitochondria-enriched fractions. Then, using mass spectrometry, we identified the following proteins as markedly oxidised in *Abcd1*$^{-}$ samples: α- and β-ATP synthase (Complex V of the OXPHOS), cytochrome b-c1 complex subunit 2 (Complex III of the OXPHOS), aspartate aminotransferase (AST) and the voltage dependent anion channel (VDAC) (Fig. 1A, 1B). In addition, the TCA cycle enzymes malate dehydrogenase (MDH) and aconitase (ACO2), the latter of which was previously detected in whole spinal cord extracts (18), showed increased levels of oxidation. These results suggest an increase in oxidative damage in *Abcd1*$^{-}$ spinal cords that affects key enzymes involved in mitochondrial energetic metabolism and confirmed that mitochondrial proteins are direct targets of oxidative lesions in spinal cords of the X-ALD mouse model.

**Oxidative phosphorylation is impaired in the spinal cord of *Abcd1*$^{-}$ mice**

Several reports indicate that the oxidation of enzymes involved in energy metabolism may result in a decrease in their activity (21). To investigate whether OXPHOS activity is altered in X-ALD mice nervous tissue, we carried out high-resolution respirometry experiments using Oroboros technology (29). Because a previous study reported no impairment in respiratory efficacy when working with purified mitochondria from muscle of an X-ALD mouse model (30), we sought to focus

on the spinal cord, the main disease target organ, and applied an *ex-vivo* approach using freshly sectioned slices from presymptomatic 12-month-old *Abcd1*$^{-}$ mice and control littermates.

Maximum oxygen consumption rates of spinal cords were assessed in the presence of the mitochondrial uncoupler carbonyl cyanide-p-trifluoromethoxyphenylhydrazone (FCCP), showing no significant differences in the activity of complexes of the ETC between both phenotypes (Fig. 2). Inhibition of Complex III of the ETC with antimycin A almost completely abolished oxygen consumption in spinal cords of both WT and *Abcd1*$^{-}$ mice (Fig. 2), strongly supporting the specificity of the oxygen consumption assay in permeabilized spinal cord slices. However, we noted that oxygen consumption after the addition of ADP, ADP + succinate or ADP + succinate + rotenone was significantly diminished in *Abcd1*$^{-}$ mice when compared to controls (Fig. 2). These results evidence that the activity of the $H^{+}$-ATP synthase is reduced in the spinal cords of *Abcd1*$^{-}$ mice, while activity of the respiration complexes remains conserved.

**C26:0 excess induces inefficient oxidative phosphorylation in X-ALD patients' fibroblasts**

To investigate whether an excess of C26:0 could be responsible for the observed mitochondrial dysfunction, we studied X-ALD patients' fibroblasts using the Seahorse Extracellular flux analyzer (XL24). This device is designed to measure oxygen consumption rates in adherent cells, allowing evaluation of cellular bioenergetics such as Oligomycin Sensitive Respiration (OSR), which is indicative of the activity of the mitochondrial $H^{+}$-ATP synthase, and the Maximum Respiratory Capacity (MRC) after

the addition of the uncoupler 2,4-dinitrophenol (DNP), which is indicative of maximum activity of the respiratory chain (31, 32).

Fibroblasts grown in glucose produce their ATP principally by glycolysis, largely by-passing the mitochondria. However, when the same cells are grown in glucose-free medium containing galactose, they are forced to raise the activity of OXPHOS system to produce ATP (33, 34). Consistent with this, OSR of both control and X-ALD fibroblasts determined in galactose media, were significantly increased when compared to the rates assayed in glucose media (Fig. 3A). Of note, control and X-ALD fibroblasts showed the same OSR when grown in glucose or galactose media (Fig. 3A), indicating a conserved activity of OXPHOS in fibroblasts of X-ALD patients under these conditions. Moreover, no differences were observed in the normalized maximum respiratory rates between control and X-ALD fibroblasts when grown in glucose or galactose media (Fig. 3B), indicating normal activity of the respiratory chain.

We next investigated the effect of excess of C26:0 upon OSR capacity. The OSR of control fibroblasts was not affected in both glucose and galactose media (Fig. 3A). Likewise, the normalized maximum respiratory rate was not affected by incubation with C26:0 (Fig. 3B). However, C26:0-treated X-ALD fibroblasts in both glucose and galactose conditions showed a diminished activity of oxidative phosphorylation (Fig. 3A), supporting that C26:0 excess may interfere with this specific mitochondrial activity in the patients' fibroblasts. The negative effect of C26:0 was also noted in the maximum respiratory rate in X-ALD fibroblasts when grown in galactose (Fig. 3B), unveiling a mitochondrial OXPHOS disruption induced by C26:0, which can be ascribed to a lower ATP synthase activity rather than lower respiratory complex activities. This is consistent with the results obtained on spinal cord slices.

We have previously observed that X-ALD fibroblasts, but not control cells, accumulate oxidative lesions to proteins in the presence of C26:0 (14). This may suggest that OSR diminution in X-ALD fibroblasts reflects C26:0-induced severe oxidation or impairment of OXPHOS subunits provoking the drop in oxidative phosphorylation activity, as revealed in the spinal cord of *Abcd1*$^{-}$ mice.

**The uncoupling of the oxidative phosphorylation or the inhibition of complexes I and II blocks free radical production**

Using the probe carboxy-$H_2$DCFDA (dichlorofluorescein), which detects reactive oxygen species (ROS) of any intracellular origin, we formerly reported that an excess of C26:0 produced oxidative lesions in proteins and generated ROS (14). However the origin of these ROS is still unknown. Because mitochondria constitute the main source of ROS in many pathological conditions (35), and our results indicated impaired oxidative phosphorylation, we sought to investigate whether also in X-ALD, mitochondria would represent a main source of ROS. We thus used the fluorescent dyes DHE (dihydroethidium) and MitoSOX (DHE covalently bonded to hexyl triphenylphosphonium cation), which measure intracellular and intra-mitochondrial ROS levels, respectively (36). The levels of ROS induced by C26:0, detected using either DHE or MitoSOX probes, were similar (Fig. 4A). This indicates that mitochondria are major sources of ROS when fibroblasts are loaded with excess of C26:0. Similar results using the MitoSOX probe were observed by Baarine *et al*. after incubating a murine transformed oligodendrocyte cell line (518N) with C26:0 and other VLCFAs (37).

As to the molecular sources of these ROS, we hypothesized that the ROS induced by C26:0 could be derived from the ETC because C26:0 somehow disrupts

oxidative phosphorylation in X-ALD fibroblasts. We thus employed different compounds that disrupt the oxidative phosphorylation in control and X-ALD fibroblasts. We observed that C26:0-mediated ROS generation was prevented when the ETC flow was uncoupled by the application of carboxy-carbonyl cyanide m-chlorophenylhydrazone (CCCP) (Fig. 4B). In addition, when Complex V was inhibited by oligomycin, we also observed the prevention of C26:0-mediated ROS production (Fig. 4C). These results highlight the mitochondrial OXPHOS system as the main molecular source of ROS induced by C26:0 and support the role played by the activity of the $H^+$-ATP synthase as a ROS-signalling cellular device (38). Of note, two subunits of this enzyme are markedly oxidized in spinal cords of the mouse model of X-ALD (Fig. 1A, 1B).

We furthermore investigated whether the inhibition of ETC complex I by rotenone and complex II by thenoyltrifluoroacetone (TTFA) (39) could lead to an alteration in the process of C26:0-mediated ROS generation. Indeed, the joint inhibition of both complexes I and II prevented C26:0-induced ROS (Fig. 4D). In contrast, no effects on C26:0-mediated ROS production were observed following complex III inhibition by antimycin (Supplementary Fig. 1A), or after the inhibition of NADPH oxidases by apocynin (Supplementary Fig. 1B) or the inhibition of cytochrome P450 by metyrapone (Supplementary Fig. 1C). Altogether, these results suggest that the C26:0-mediated ROS generation is produced by the ETC, with evidence that complexes I and II may most likely constitute the main sources of ROS upon C26:0 excess in this cellular system. These results are in agreement with the reduced OSR observed in X-ALD fibroblasts in presence of C26:0 overload, which suggests that C26:0 may hamper by an unknown mechanism the correct electron transport, facilitating electron leakage, and thus decreasing the phosphorylative respiration in these cells (Fig. 3A).

**Mitochondrial DNA is oxidised in cerebral AMN brain samples and in human fibroblasts after C26:0 exposure**

Compared to nuclear DNA, mitochondrial DNA is more sensitive to mutations caused by oxidative stress because of certain factors that include a lack of protective histones and the close proximity of the mitochondrial genome to the inner mitochondrial membrane where ROS are produced (40). To investigate whether an excess of C26:0 was able to generate mtDNA damage, we measured mtDNA oxidation levels by means of a Q-PCR approach. This is based on the fact that PCR efficiency is directly correlated to DNA oxidation levels (41), i.e. unlike that of a small DNA fragment (100 bp), the PCR efficiency of large DNA fragments (1 kb) is diminished by oxidation as deletions occur. Thus, the difference in PCR efficiency between a small and a large DNA fragment in the same locus allows us to measure the number of oxidised bases/kb. We applied this technique to samples of brain white matter of human adrenomyeloneuropathy patients, and detected increased mtDNA oxidation ratios in the affected white matter zones, which show active demyelinising plaques (Fig 5A). To investigate whether excess of C26:0 could be responsible for this effect, we used human fibroblasts and exposed the cells to excess of C26:0, showing that both control and X-ALD cells had increased oxidation rates under these conditions (Fig. 5B). Taken together, our data support the hypothesis that an excess of C26:0 triggers a vicious cycle of mitochondrial dysfunction that may constitute the initial steps in the neurodegenerative cascade in this disease.

## DISCUSSION

Oxidative stress has been classically considered to be a common event in the neurodegenerative cascade in a variety of conditions (20, 21). Moreover mitochondria, and in particular the ETC, have been identified as main sources of ROS in many neurodegenerative diseases (35). The leakage of electrons from the electron transport chain located on the inner mitochondrial membrane is the source of superoxide $O_2^{\cdot -}$, which then produces $H_2O_2$ by dismutation (42). ROS are extremely reactive molecules that oxidise nearby macromolecules in the absence of the antioxidant defence system (43). This oxidation can induce mutations in DNA and structural and functional modifications to proteins and lipids, increasing a pathological cascade of molecular damage that, if not neutralized, may lead to cellular demise.

A main conclusion of this study is that an excess of C26:0 disrupts the mitochondrial oxidative phosphorylation and induces the generation of free radicals at the ETC, in particular when oxido-reduction reactions take place in both complexes I and II, at least in human fibroblasts. This in turn may lead to ETC malfunctioning and defective phosphorylative respiration evidenced *in vitro* in fibroblasts and *ex-vivo* using spinal cord slices of presymptomatic X-ALD mice. Thus, we propose that an oxidatively damaged and functionally impaired OXPHOS system may be at the sources of the neurodegenerative cascade in X-ALD. This hypothesis is consistent with previous findings studying neurodegenerative models. HD patients show a decrease in the activity of complex I in skeletal muscle, and complexes II/III and IV in the brain (44). The activity of complex I in the substantia nigra and in the frontal cortex of PD patients is also reduced. In addition, complex IV activity is decreased in the hippocampus of AD patients (45). Moreover, it has been demonstrated that both the inhibition of complex I by 1-methyl-4-phenyl- 1,2,3,6-tetrahydropyridine (MPTP) and complex II by 3-

nitropropionic acid (3-NP) in rodents leads to PD and HD, respectively (46, 47). Our data appear to be in contrast with previous research in the field showing that respiration in isolated mitochondria from the muscle of an *Abcd1*$^{-}$ mouse was normal (30). As the muscle is not an organ primarily affected in the disease, one possible explanation could be that mitochondria susceptibility to VLCFA excess may vary among tissues and cell types, as the functions of these organelles may show a certain degree of heterogeneity and super-specialization among populations to adapt to specific demands and physiological functions.

Moreover, as a logical consequence of excessive mitochondrial ROS production, we also identified an increase in oxidised mtDNA and mitochondrial proteins of TCA cycle and OXPHOS in X-ALD nervous tissues. Of note, the oxidised molecules observed in X-ALD have already been identified in several neurodegenerative disorders including mtDNA in the brains of patients with AD (48) and HD (49); VDAC1 and α- and β-ATP synthase in AD (21, 50); aconitase in AD and HD (21); aspartate aminotransferase in a HD mouse model (51); and cytochrome b-c1 oxidation in the frontal cerebral cortex of advanced AD (43). This may be one underlying reason for the bioenergetic deficiency common to all these neurodegenerative diseases, and provide the rationale for exchange of therapeutic strategies among these pathologies (17).

The precise molecular mechanisms that may drive the noxious interaction of C26:0 with mitochondria membranes and thus, the excessive mitochondria-derived ROS production in the context of X-ALD remains obscure at present. It is worth noting that the accumulation of fatty acids causes the mitochondria dysfunction underlying both common and rare conditions, such as type 2 diabetes or Refsum disease (52-54). Because it has been shown that C26:0 can interact with a phospholipid bilayer membrane provoking a perturbation of bilayer organisation (55-57), it is conceivable

that an excess of C26:0, perhaps substituting other fatty acid species, namely polyunsaturated or monounsaturated fatty acids at the lateral chains of membrane phospholipids, could interfere with mitochondrial membrane structure and fluidity, which would disturb the proper physical interaction of OXPHOS subunits and facilitate electron leakage. These ROS would then attack fatty acid anions and produce lipid peroxides, which are highly reactive and could lead to oxidative damage to DNA, RNA and enzymes of the membrane such as the ATP synthase, or the matrix, which in turn would lead to structural damage to mitochondria. As a consequence, the inner membrane potential would decrease along with the ETC inefficiency and ROS production reported here (Fig.6). The elucidation of the more precise molecular mechanism should be addressed in future studies.

Taken together, our results indicate that an excess of C26:0 induces mitochondrial dysfunction in X-ALD by producing: i) mitochondrial ROS, ii) mitochondrial oxidative damage to DNA and proteins, and iii) inefficient oxidative phosphorylation (Fig. 6). The mechanism appears to be the excessive generation of mitochondrial ROS through the chronic accumulation of C26:0, which irrevocably exacerbates mitochondrial dysfunction and leads to cell demise. In summary, our present study underscores the critical role of impaired mitochondria respiration and bioenergetics in the pathogenesis of X-ALD, which is of great importance for the clinical management of X-ALD patients. Furthermore, our results spotlight an oxidative phosphorylation impairment early in the physiopathological cascade underlying axonal degeneration and thus, pave the road for new therapeutic strategies using new-generation antioxidants targeted to mitochondria. This may be of relevance for other neurodegenerative diseases presenting mitochondrial dysfunction and for metabolic conditions caused by the accumulation of very long-chain saturated fatty acids that are

potentially toxic to this vital organelle.

## MATERIAL AND METHODS

### Material

The following chemicals were used: 6-carboxy-2', 7'-dichlorodihydrofluorescein diacetate, diacetoxymethyl ester ($H_2$DCFDA)(Molecular probes); dihydroethidium (DHE) (Molecular Probes) ; MitoSOX (Molecular Probes) ; hexacosanoic acid (C26:0)(Sigma) ; CCCP (Sigma) ; FCCP (Sigma) ; oligomycin (Sigma) ; antimycin A (Sigma) ; rotenone (Sigma) ; thenoyltrifluoroacetone (TTFA) (Sigma) ; apocynin (Sigma) ; metyrapone (Sigma) ; N,N,N',N'-tetramethyl-p-phenylenediamine (TMPD) (Sigma).

### Antibodies

The following antibodies were used for western blots: anti-DNP: dilution 1/100 (Invitrogen) as primary antibody and goat anti-rabbit IgG linked to horseradish peroxidase, dilution: 1/15000 (P0448, Dako, Glostrup, Denmark) as secondary antibody.

### Cell Culture and Treatments

Control and X-ALD human fibroblasts were grown as described (14). Control (n=7) and X-ALD human fibroblasts (n=9) were treated in medium containing fetal bovine serum (10%) for 24 hours with ethanol as control, C26:0 (50μM), or an inhibitor with C26:0 (50μM). The following battery of inhibitors was used: CCCP (10μM), oligomycin (8μM), rotenone (10nM), TTFA (500μM), antimycin A (1μM), apocynin (ranges from 50 to 300μM, higher doses produced cell lethality) metyrapone (ranges

from 50 to 500μM, higher doses produced cell lethality). Experiments were carried out with cells at 80-90% of confluence, which had a number of passages ranging from 12 to 15.

**Mouse breeding**

The generation and genotyping of *Abcd1*$^{-}$ mice has previously been described (9, 10, 58). Mice used for experiments were of a pure C57BL/6J background. Males were sacrificed and tissues were recovered and conserved at −80°C. All methods employed in this study were in accordance with the Guide for the Care and Use of Laboratory Animals published by the US National Institutes of Health (NIH Publications No. 85–23, revised 1996) and with the ethical committee of The Bellvitge Institute of Biomedical Research and the government of Catalonia.

**Human brain samples**

Brain tissues from cerebral X-linked adrenoleukodystrophy patients and healthy male control subjects, age matched, were obtained from the Brain and Tissue Bank for Developmental Disorders at the University of Maryland, Baltimore, MD, USA as described in (28). Four clinically diagnosed cALD (cerebral childhood ALD) patients and five cAMN (cerebral adrenomyeloneuropathy) patients were used. Informed written consent was obtained from all patients or their legal representatives and the local ethics committee.

**Mitochondrial DNA damage**

Mitochondrial DNA oxidation level was quantified by a Q-PCR approach has earlier reported (41).

**Two-dimensional electrophoresis and western blotting**

Redox proteomics for the identification of oxidised proteins in mice spinal cords and human fibroblasts were performed as previously described (18).

**Mitochondria enrichment**

Fifty mg of fresh spinal cord is homogenized in 1mL of ice-cold sucrose buffer (sucrose 0.32M, HEPES 4mM pH7.4 and protease inhibitor cocktail) using a dounce with tight pestle and centrifuged 10min at 1000g in a refrigerated microcentrifuge. The supernatant (S1a) is kept in ice and the pellet resuspended in 750 µl of ice-cold sucrose buffer, then centrifuged 10min at 1000g in a refrigerated microcentrifuge. The supernatant (S1b) is kept in ice and the pellet resuspended in 750 µl of ice-cold sucrose buffer, then centrifuged 10min at 1000g in a refrigerated microcentrifuge. The supernatant (S1c) is kept in ice and the pellet discarded. S1a, S1b and S1c are centrifuged at 16000g for 10min in a refrigerated microcentrifuge. The pellet contains the mitochondrial and lysosomal enriched fractions.

**Evaluation of intracellular ROS**

Intracellular ROS levels were estimated using different ROS-sensitive fluorescent probes ($H_2$DCFDA) excepted when it is specified in the figure legend as described (14). $H_2$DCFDA and DHE probes were used to quantify intracellular ROS. MitoSOX™ Red (Molecular Probes) was used to quantify intra-mitochondrial ROS. Following incubation with 10 µM $H_2$DCFDA for 30 min, 5 µM DHE for 30 min or 5 µM MitoSox for 10 min, cells were washed twice with PBS and lysed with 1% Triton X-100 (10 min, 4ºC). The homogenate was transferred into a 96-well plate for

fluorescence detection with a spectrofluorimeter. Wavelength filters used were: exc. 485 nm, em. 520 nm for $H_2$DCFDA and exc. 530 nm, em. 590 nm for DHE and MitoSOX. Fluorescence values were corrected with protein content and results were expressed as percentage to control (untreated cells).

**Oxygen consumption rate using Seahorse**

Oxygen consumption rate (OCR) in adherent fibroblasts was measured in control and X-ALD fibroblasts with a XF24 Extracellular Flux Analyzer (Seahorse Bioscience, Billerica, MA, USA). Fibroblasts were cultured in 12 wells of a XF 96-well cell culture microplate (Seahorse Bioscience) at a density of $15\times10^3$ cells/well in 100 µL of growth medium (DMEM with pyruvate, 1g/L of glucose and 10% de FBS). After 3 h, 150 µL of growth medium was added and cell were kept at 37 °C and 5 % $CO_2$ atmosphere. The next day growth medium was replaced with a glucose-free DMEM containing 2mM of L-glutamate, 10% of FBS and 1g/L of glucose. C26:0 (50 µM) or EtOH was added in the medium, and then cells were incubated for 30h at 37 °C in 5% $CO_2$ atmosphere. The cells were incubated at 37°C for 60 min to allow media temperature and pH to reach equilibrium before the first rate measurement. After an OCR baseline measurement, 50 µL of oligomycin and dinitrophenyl (DNP) were sequentially added to each well to reach working concentrations of 6 µM and 500 µM respectively and changes in the OCR were analyzed. Oligomycin sensitive respiration (OSR) values were calculated from the differences between the baseline OCR and the OCR after oligomycin inhibition. Data were expressed as pmol of $O_2$ per minute per 15000 cells. Mitochondrial maximum respiratory capacity values were obtained from the ratio between baseline OCR and the OCR after the addition of the uncoupler DNP. All determinations were performed in 7 control and 9 X-ALD fibroblasts.

**High resolution respirometry using Oroboros**

Oxygen flux of sets of 5 permeabilized slices of spinal cord per mouse (n=4 mice per genotype) was measured at 37 °C in MiR05 medium (pH 7.4) by high-resolution respirometry using the Oroboros® Oxygraph-2k with chamber volumes set at 2 mL and at a slow stirring speed (150 rpm) in order to avoid tissue disaggregation. DatLab software (Oroboros Instruments, Innsbruck, Austria) was used for data acquisition (2 s time intervals) and analysis, which includes calculation of the time derivative of oxygen concentration and correction for instrumental background oxygen flux (59). The spinal cord slices permeabilization protocol was a modification of a previously published method (60). Fresh spinal cords were rinsed with ice-cold normal saline and cut into slices with a tissue chopper adjusted to a cut width of 300 mm. About 12-15 slices of the lumbar region were collected and transferred quickly into individual wells of a 6-well tissue culture plate with 2 ml of ice-cold permeabilization medium (in mM: 7.23 potassium ethylene glycol-bis(b-aminoethyl ether)*N*,*N*,*N'*,*N'*-tetraacetate ($K_2$ EGTA), 2.77 $CaK_2$ EGTA, 60 *N*,*N*-bis[2-hydroxyethyl]- 2-aminoethanesulfonic acid (BES), 5.69 MgATP, 20 taurine, 3 $K_2HPO4$ , 0.5 dithiothreitol and 81 potassium methanesulfonate, pH 7.1 at 25°C), rinsed and immediately transferred again into another well with the same medium containing 20 µl of saponin stock solution (5 mg/ml; final concentration 50 µg/ml). Spinal cord slices were shaken by gentle agitation in the cold room (on ice) for 30 min. After the 30 min period, all samples are quickly transferred from the saponin permeabilization medium into 2 ml of respiration medium (in mM: 7.23 $K_2$ EGTA, 2.77 $CaK_2$ EGTA, 100 potassium salt of 2-(N-morpholino)ethanesulfonic acid (K-MES), 1.38 $MgCl_2$ , 20 taurine, 3 $K_2HPO4$ , 0.5 dithiothreitol, 20 imidazole and 5 mg/ml bovine serum albumine (BSA), pH 7.1 at 25ºC), and shaken by gentle agitation

for 10 min in the cold room (on ice). For evaluation of relative contributions of mitochondrial complexes to oxygen consumption, several specific mitochondrial poisons and substrates (rotenone, antimycin A, carbonyl cyanide-p-trifluoromethoxyphenylhydrazone (FCCP) and N,N,N',N'-tetramethyl-p-phenylenediamine (TMPD)) were used as previously described (59) and calculated as steady-state respiratory flux in the time interval between 5 and 10 min after its addition. In order to avoid oxygen limitations, all the experiments were performed above 50% oxygen saturation. Initially, we measured endogenous respiration in the absence of exogenous substrates. We proceeded to sequentially analyse the activities of the ETC complexes. First, we added glutamate and malate to increase NADH levels in order to measure the complex I non-phosphorylative activity, or state 2. ADP was added to quantify the complex I-dependent phosphorylative activity, or state 3. Immediately afterwards, we added succinate, which is the substrate for complex II. At this point, the level of $O_2$ consumption corresponded to complex I- and II-dependent phosphorylative activity. The addition of rotenone inhibits complex I; therefore, $O_2$ consumption measured after the addition of rotenone only reflects complex II-dependent phosphorylative activity. Then, complex III activity was inhibited with antimycin A, and finally Complex IV maximal activity was measured after addition of the non-physiological substrate *N*,*N*,*N*',*N*'-tetramethyl-*p*-phenylenediamine (TMPD). Maximum oxygen consumption rates of spinal cords were measured after addition of FCCP. Oxygen consumption was normalized by actual protein content in the respirometer chambers.

**Statistical analysis**

Data are given as mean +/- SD. Significant differences were determined by Student's t-test or one-way ANOVA followed by Tukey's HSD post hoc (* $P$ <0.05, ** $P$<0.01, *** $P$<0.001) after verifying normality. Statistical analyses were performed using SPSS 12.0 program.

**ACKNOWLEDGEMENTS**

We express our gratitude to the Brain and Tissue Bank for Developmental Disorders at the University of Maryland for supplying the case material used in the human studies. This study was supported by grants from the European Commission [FP7-241622], the European Leukodystrophy Association [ELA2009-036C5; ELA2008-040C4], the Spanish Institute for Health Carlos III [FIS PI080991 and FIS PI11/01043], the Autonomous Government of Catalonia [2009SGR85] to A.P and the Spanish Institute for Health Carlos III [Miguel Servet program CP11/00080] to S.F. The CIBER on Rare Diseases (CIBERER) is an initiative of the ISCIII. The study was developed under the COST action BM0604 [to A.P.]. J.L-E. was a fellow of the Department of Education, Universities and Research of the Basque Country Government (BFI07.126). S.F. was a fellow of the European Leukodystrophy Association [ELA 2010-020F1]. L.M. is a fellow of the Spanish Ministry of Education [FPU program: AP2008-03728].

The studies conducted at the Department of Experimental Medicine were supported in part by R+D grants from the Spanish Ministry of Science and Innovation [BFU2009-11879/BFI], the Spanish Ministry of Health [PI11/1532], the Autonomous Government of Catalonia [2009SGR735], the 'La Caixa' Foundation and COST B35 Action of the European Union. D.C. is a fellow from Spanish Ministry of Health [FI08-

00707]. The studies conducted at the Department of Biochemistry and Molecular Biology, University of Barcelona, were supported by grants SAF2008-01896 and SAF2011-23636 from the Spanish Ministry of Science and Innovation.

The CIBER in Physiopathology of Obesity and Nutrition (CIBERobn) is an initiative of the ISCIII.

## CONFLICT OF INTEREST

The authors declare that they have no conflict of interest.

**Abbreviations:** 3NP = 3-nitropropionic acid; ACO2 = aconitase; AD = Alzheimer's disease; AMN = adrenomyeloneuropathy; AST = aspartate aminotransferase; cALD = cerebral childhood ALD; cAMN = cerebral adrenomyeloneuropathy; CCCP = carboxy-carbonyl cyanide m-chlorophenylhydrazone; DHE = dihydroethidium; DNP = 2,4-dinitrophenol; ETC = electron transport chain; FCCP = carbonyl cyanide-p-trifluoromethoxyphenylhydrazone; HD = Huntington's disease; MDH = malate dehydrogenase; MPTP = 1-methyl-4-phenyl-1,2,3,6-tetrahydropyridine; MRC = Maximum Respiratory Capacity; mtDNA = mitochondrial DNA; OCR = oxygen consumption rate; OSR = Oligomycin Sensitive Respiration; OXPHOS = oxidative phosphorylation; PD = Parkinson's Diseases; ROS = reactive oxygen species; TCA = tricarboxylic acid cycle; TMPD = *N*,*N*,*N'*,*N'*-tetramethyl-*p*-phenylenediamine; TTFA = thenoyltrifluoroacetone; X-ALD = X-linked adrenoleukodystrophy; VLCFA = very long-chain fatty acid; VDAC = voltage dependent anion channel; WT = wild type.

## REFERENCES


1. Ferrer, I., Aubourg, P. and Pujol, A. (2010) General aspects and neuropathology of X-linked adrenoleukodystrophy. *Brain Pathol,* 20, 817-30.
2. Moser, H., Smith, KD, Watkins, PA, Powers, J, Moser, AB (2001) X-linked adrenoleukodystrophy. In Scriver, C. (ed.), *The Metabolic and Molecular Bases of Inherited disease.* 8th ed. McGraw-Hill, New-York, Vol. II, pp. 3257-3301.
3. Powers, J.M., DeCiero, D.P., Ito, M., Moser, A.B. and Moser, H.W. (2000) Adrenomyeloneuropathy: a neuropathologic review featuring its noninflammatory myelopathy. *J Neuropathol Exp Neurol,* 59, 89-102.
4. Mosser, J., Douar, A.M., Sarde, C.O., Kioschis, P., Feil, R., Moser, H., Poustka, A.M., Mandel, J.L. and Aubourg, P. (1993) Putative X-linked adrenoleukodystrophy gene shares unexpected homology with ABC transporters. *Nature,* 361, 726-730.
5. van Roermund, C.W., Visser, W.F., Ijlst, L., van Cruchten, A., Boek, M., Kulik, W., Waterham, H.R. and Wanders, R.J. (2008) The human peroxisomal ABC half transporter ALDP functions as a homodimer and accepts acyl-CoA esters. *Faseb J,* 22, 4201-8.
6. Fourcade, S., Ruiz, M., Camps, C., Schluter, A., Houten, S.M., Mooyer, P.A., Pampols, T., Dacremont, G., Wanders, R.J., Giros, M. *et al.* (2009) A key role for the peroxisomal ABCD2 transporter in fatty acid homeostasis. *Am J Physiol Endocrinol Metab,* 296, E211-21.
7. Singh, I., Moser, A.E., Moser, H.W. and Kishimoto, Y. (1984) Adrenoleukodystrophy: impaired oxidation of very long chain fatty acids in white blood cells, cultured skin fibroblasts, and amniocytes. *Pediatr Res,* 18, 286-90.
8. Wanders, R.J., van Roermund, C.W., van Wijland, M.J., Nijenhuis, A.A., Tromp, A., Schutgens, R.B., Brouwer-Kelder, E.M., Schram, A.W., Tager, J.M., van den Bosch, H. *et al.* (1987) X-linked adrenoleukodystrophy: defective peroxisomal oxidation of very long chain fatty acids but not of very long chain fatty acyl-CoA esters. *Clin Chim Acta,* 165, 321-9.
9. Pujol, A., Ferrer, I., Camps, C., Metzger, E., Hindelang, C., Callizot, N., Ruiz, M., Pampols, T., Giros, M. and Mandel, J.L. (2004) Functional overlap between ABCD1 (ALD) and ABCD2 (ALDR) transporters: a therapeutic target for X-adrenoleukodystrophy. *Hum.Mol.Genet.,* 13, 2997-3006.
10. Pujol, A., Hindelang, C., Callizot, N., Bartsch, U., Schachner, M. and Mandel, J.L. (2002) Late onset neurological phenotype of the X-ALD gene inactivation in mice: a mouse model for adrenomyeloneuropathy. *Hum Mol Genet,* 11, 499-505.
11. Fourcade, S., Ruiz, M., Guilera, C., Hahnen, E., Brichta, L., Naudi, A., Portero-Otin, M., Dacremont, G., Cartier, N., Wanders, R. *et al.* (2010) Valproic acid induces antioxidant effects in X-linked adrenoleukodystrophy. *Hum Mol Genet,* 19, 2005-14.
12. Powers, J.M., Pei, Z., Heinzer, A.K., Deering, R., Moser, A.B., Moser, H.W., Watkins, P.A. and Smith, K.D. (2005) Adreno-leukodystrophy: oxidative stress of mice and men. *J Neuropathol Exp Neurol,* 64, 1067-79.
13. Vargas, C.R., Wajner, M., Sirtori, L.R., Goulart, L., Chiochetta, M., Coelho, D., Latini, A., Llesuy, S., Bello-Klein, A., Giugliani, R. *et al.* (2004) Evidence that oxidative stress is increased in patients with X-linked adrenoleukodystrophy. *Biochim Biophys Acta,* 1688, 26-32.
14. Fourcade, S., Lopez-Erauskin, J., Galino, J., Duval, C., Naudi, A., Jove, M., Kemp, S., Villarroya, F., Ferrer, I., Pamplona, R. *et al.* (2008) Early oxidative damage underlying neurodegeneration in X-adrenoleukodystrophy. *Hum Mol Genet,* 17, 1762-73.
15. Lopez-Erauskin, J., Galino, J., Bianchi, P., Fourcade, S., Andreu, A.L., Ferrer, I., Munoz-Pinedo, C. and Pujol, A. (2012) Oxidative stress modulates mitochondrial failure and cyclophilin D function in X-linked adrenoleukodystrophy. *Brain,* 135, 3584-98.
16. Singh, I. and Pujol, A. (2010) Pathomechanisms underlying X-adrenoleukodystrophy: a three-hit hypothesis. *Brain Pathol,* 20, 838-44.

17. Galea, E., Launay, N., Portero-Otin, M., Ruiz, M., Pamplona, R., Aubourg, P., Ferrer, I. and Pujol, A. (2012) Oxidative stress underlying axonal degeneration in adrenoleukodystrophy: A paradigm for multifactorial neurodegenerative diseases? *Biochim Biophys Acta*.
18. Galino, J., Ruiz, M., Fourcade, S., Schluter, A., Lopez-Erauskin, J., Guilera, C., Jove, M., Naudi, A., Garcia-Arumi, E., Andreu, A.L. *et al.* (2011) Oxidative damage compromises energy metabolism in the axonal degeneration mouse model of x-adrenoleukodystrophy. *Antioxid Redox Signal,* 15, 2095-107.
19. Lopez-Erauskin, J., Fourcade, S., Galino, J., Ruiz, M., Schluter, A., Naudi, A., Jove, M., Portero-Otin, M., Pamplona, R., Ferrer, I. *et al.* (2011) Antioxidants halt axonal degeneration in a mouse model of X-adrenoleukodystrophy. *Ann Neurol,* 70, 84-92.
20. Lin, M.T. and Beal, M.F. (2006) Mitochondrial dysfunction and oxidative stress in neurodegenerative diseases. *Nature,* 443, 787-95.
21. Martinez, A., Portero-Otin, M., Pamplona, R. and Ferrer, I. (2010) Protein targets of oxidative damage in human neurodegenerative diseases with abnormal protein aggregates. *Brain Pathol,* 20, 281-97.
22. Ferrer, I., Kapfhammer, J.P., Hindelang, C., Kemp, S., Troffer-Charlier, N., Broccoli, V., Callyzot, N., Mooyer, P., Selhorst, J., Vreken, P. *et al.* (2005) Inactivation of the peroxisomal ABCD2 transporter in the mouse leads to late-onset ataxia involving mitochondria, Golgi and endoplasmic reticulum damage. *Hum Mol Genet,* 14, 3565-77.
23. McGuinness, M.C., Lu, J.F., Zhang, H.P., Dong, G.X., Heinzer, A.K., Watkins, P.A., Powers, J. and Smith, K.D. (2003) Role of ALDP (ABCD1) and mitochondria in X-linked adrenoleukodystrophy. *Mol Cell Biol,* 23, 744-53.
24. Powers, J.M., DeCiero, D.P., Cox, C., Richfield, E.K., Ito, M., Moser, A.B. and Moser, H.W. (2001) The dorsal root ganglia in adrenomyeloneuropathy: neuronal atrophy and abnormal mitochondria. *J Neuropathol Exp Neurol,* 60, 493-501.
25. Schroder, J.M., Mayer, M. and Weis, J. (1996) Mitochondrial abnormalities and intrafamilial variability of sural nerve biopsy findings in adrenomyeloneuropathy. *Acta Neuropathol,* 92, 64-9.
26. Goldfischer, S., Moore, C.L., Johnson, A.B., Spiro, A.J., Valsamis, M.P., Wisniewski, H.K., Ritch, R.H., Norton, W.T., Rapin, I. and Gartner, L.M. (1973) Peroxisomal and mitochondrial defects in the cerebro-hepato-renal syndrome. *Science,* 182, 62-4.
27. Baumgart, E., Vanhorebeek, I., Grabenbauer, M., Borgers, M., Declercq, P.E., Fahimi, H.D. and Baes, M. (2001) Mitochondrial alterations caused by defective peroxisomal biogenesis in a mouse model for Zellweger syndrome (PEX5 knockout mouse). *Am J Pathol,* 159, 1477-94.
28. Schluter, A., Espinosa, L., Fourcade, S., Galino, J., Lopez, E., Ilieva, E., Morato, L., Asheuer, M., Cook, T., McLaren, A. *et al.* (2012) Functional genomic analysis unravels a metabolic-inflammatory interplay in adrenoleukodystrophy. *Hum Mol Genet,* 21, 1062-77.
29. Singh, I.N., Sullivan, P.G., Deng, Y., Mbye, L.H. and Hall, E.D. (2006) Time course of post-traumatic mitochondrial oxidative damage and dysfunction in a mouse model of focal traumatic brain injury: implications for neuroprotective therapy. *J Cereb Blood Flow Metab,* 26, 1407-18.
30. Oezen, I., Rossmanith, W., Forss-Petter, S., Kemp, S., Voigtlander, T., Moser-Thier, K., Wanders, R.J., Bittner, R.E. and Berger, J. (2005) Accumulation of very long-chain fatty acids does not affect mitochondrial function in adrenoleukodystrophy protein deficiency. *Hum Mol Genet,* 14, 1127-37.
31. Moran, M., Rivera, H., Sanchez-Arago, M., Blazquez, A., Merinero, B., Ugalde, C., Arenas, J., Cuezva, J.M. and Martin, M.A. (2010) Mitochondrial bioenergetics and dynamics interplay in complex I-deficient fibroblasts. *Biochim Biophys Acta,* 1802, 443-53.
32. Wu, M., Neilson, A., Swift, A.L., Moran, R., Tamagnine, J., Parslow, D., Armistead, S., Lemire, K., Orrell, J., Teich, J. *et al.* (2007) Multiparameter metabolic analysis reveals a

close link between attenuated mitochondrial bioenergetic function and enhanced glycolysis dependency in human tumor cells. *Am J Physiol Cell Physiol,* 292, C125-36.
33. Hofhaus, G., Johns, D.R., Hurko, O., Attardi, G. and Chomyn, A. (1996) Respiration and growth defects in transmitochondrial cell lines carrying the 11778 mutation associated with Leber's hereditary optic neuropathy. *J Biol Chem,* 271, 13155-61.
34. Robinson, B.H., Petrova-Benedict, R., Buncic, J.R. and Wallace, D.C. (1992) Nonviability of cells with oxidative defects in galactose medium: a screening test for affected patient fibroblasts. *Biochem Med Metab Biol,* 48, 122-6.
35. Fernandez-Checa, J.C., Fernandez, A., Morales, A., Mari, M., Garcia-Ruiz, C. and Colell, A. (2010) Oxidative stress and altered mitochondrial function in neurodegenerative diseases: lessons from mouse models. *CNS Neurol Disord Drug Targets,* 9, 439-54.
36. Mukhopadhyay, P., Rajesh, M., Yoshihiro, K., Hasko, G. and Pacher, P. (2007) Simple quantitative detection of mitochondrial superoxide production in live cells. *Biochem Biophys Res Commun,* 358, 203-8.
37. Baarine, M., Andreoletti, P., Athias, A., Nury, T., Zarrouk, A., Ragot, K., Vejux, A., Riedinger, J.M., Kattan, Z., Bessede, G. *et al.* (2012) Evidence of oxidative stress in very long chain fatty acid - Treated oligodendrocytes and potentialization of ROS production using RNA interference-directed knockdown of ABCD1 and ACOX1 peroxisomal proteins. *Neuroscience,* 213, 1-18.
38. Formentini, L., Sanchez-Arago, M., Sanchez-Cenizo, L. and Cuezva, J.M. (2012) The mitochondrial ATPase inhibitory factor 1 triggers a ROS-mediated retrograde prosurvival and proliferative response. *Mol Cell,* 45, 731-42.
39. Nadanaciva, S., Bernal, A., Aggeler, R., Capaldi, R. and Will, Y. (2007) Target identification of drug induced mitochondrial toxicity using immunocapture based OXPHOS activity assays. *Toxicol In Vitro,* 21, 902-11.
40. Pamplona, R. and Barja, G. (2007) Highly resistant macromolecular components and low rate of generation of endogenous damage: two key traits of longevity. *Ageing Res Rev,* 6, 189-210.
41. Rothfuss, O., Gasser, T. and Patenge, N. (2010) Analysis of differential DNA damage in the mitochondrial genome employing a semi-long run real-time PCR approach. *Nucleic Acids Res,* 38, e24.
42. Fridovich, I. (2004) Mitochondria: are they the seat of senescence? *Aging Cell,* 3, 13-6.
43. Pamplona, R., Dalfo, E., Ayala, V., Bellmunt, M.J., Prat, J., Ferrer, I. and Portero-Otin, M. (2005) Proteins in human brain cortex are modified by oxidation, glycoxidation, and lipoxidation. Effects of Alzheimer disease and identification of lipoxidation targets. *J Biol Chem,* 280, 21522-30.
44. Turner, C. and Schapira, A.H. (2010) Mitochondrial matters of the brain: the role in Huntington's disease. *J Bioenerg Biomembr,* 42, 193-8.
45. Fukui, H. and Moraes, C.T. (2008) The mitochondrial impairment, oxidative stress and neurodegeneration connection: reality or just an attractive hypothesis? *Trends Neurosci,* 31, 251-6.
46. Pandey, M., Mohanakumar, K.P. and Usha, R. (2010) Mitochondrial functional alterations in relation to pathophysiology of Huntington's disease. *J Bioenerg Biomembr,* 42, 217-26.
47. Winklhofer, K.F. and Haass, C. (2010) Mitochondrial dysfunction in Parkinson's disease. *Biochim Biophys Acta,* 1802, 29-44.
48. Wang, J., Xiong, S., Xie, C., Markesbery, W.R. and Lovell, M.A. (2005) Increased oxidative damage in nuclear and mitochondrial DNA in Alzheimer's disease. *J Neurochem,* 93, 953-62.
49. Polidori, M.C., Mecocci, P., Browne, S.E., Senin, U. and Beal, M.F. (1999) Oxidative damage to mitochondrial DNA in Huntington's disease parietal cortex. *Neurosci Lett,* 272, 53-6.
50. Butterfield, D.A., Poon, H.F., St Clair, D., Keller, J.N., Pierce, W.M., Klein, J.B. and Markesbery, W.R. (2006) Redox proteomics identification of oxidatively modified

hippocampal proteins in mild cognitive impairment: insights into the development of Alzheimer's disease. *Neurobiol Dis,* 22, 223-32.

51. Perluigi, M., Poon, H.F., Maragos, W., Pierce, W.M., Klein, J.B., Calabrese, V., Cini, C., De Marco, C. and Butterfield, D.A. (2005) Proteomic analysis of protein expression and oxidative modification in r6/2 transgenic mice: a model of Huntington disease. *Mol Cell Proteomics,* 4, 1849-61.
52. Reiser, G., Schonfeld, P. and Kahlert, S. (2006) Mechanism of toxicity of the branched-chain fatty acid phytanic acid, a marker of Refsum disease, in astrocytes involves mitochondrial impairment. *Int J Dev Neurosci,* 24, 113-22.
53. Schonfeld, P. and Reiser, G. (2006) Rotenone-like action of the branched-chain phytanic acid induces oxidative stress in mitochondria. *J Biol Chem,* 281, 7136-42.
54. Schrauwen, P. and Hesselink, M.K. (2004) Oxidative capacity, lipotoxicity, and mitochondrial damage in type 2 diabetes. *Diabetes,* 53, 1412-7.
55. Ho, J.K., Moser, H., Kishimoto, Y. and Hamilton, J.A. (1995) Interactions of a very long chain fatty acid with model membranes and serum albumin. Implications for the pathogenesis of adrenoleukodystrophy. *J Clin Invest,* 96, 1455-63.
56. Powers, J.M. and Moser, H.W. (1998) Peroxisomal disorders: genotype, phenotype, major neuropathologic lesions, and pathogenesis. *Brain Pathol,* 8, 101-20.
57. Theda, C., Moser, A.B., Powers, J.M. and Moser, H.W. (1992) Phospholipids in X-linked adrenoleukodystrophy white matter: fatty acid abnormalities before the onset of demyelination. *J Neurol Sci,* 110, 195-204.
58. Lu, J.F., Lawler, A.M., Watkins, P.A., Powers, J.M., Moser, A.B., Moser, H.W. and Smith, K.D. (1997) A mouse model for X-linked adrenoleukodystrophy. *Proc.Natl.Acad.Sci.U.S.A,* 94, 9366-9371.
59. Justo, R., Boada, J., Frontera, M., Oliver, J., Bermudez, J. and Gianotti, M. (2005) Gender dimorphism in rat liver mitochondrial oxidative metabolism and biogenesis. *Am J Physiol Cell Physiol,* 289, C372-8.
60. Safiulina, D., Kaasik, A., Seppet, E., Peet, N., Zharkovsky, A. and Seppet, E. (2004) Method for in situ detection of the mitochondrial function in neurons. *J Neurosci Methods,* 137, 87-95.

## FIGURE LEGENDS

**Figure 1: Mitochondrial proteins are more markedly oxidised in spinal cords of 12-month-old *Abcd1*$^{-}$ mice**

**A)** 2D-Redox proteomics of mitochondrial enriched fractions of spinal cords of 12-month-old WT and *Abcd1*$^{-}$ mice using two-dimensional gel electrophoresis. Oxidised proteins were detected using an anti-DNP antibody. Representative blots are shown (n=4 samples/genotype). **B)** List of more markedly oxidised mitochondrial proteins in spinal cords of *Abcd1*$^{-}$ mice detected by anti-DNP antibody and subsequently identified by mass spectrometry. Detailed image of identified proteins is shown (n=4 samples/genotype).

**Figure 2: Oxidative phosphorylation is diminished in *Abcd1*$^{-}$ mouse spinal cords**

Respiration analysis was performed on permeabilized sections of spinal cords of 12-month-old WT and *Abcd1*$^{-}$ mice, using an Oxygraph-2k high-resolution respirometer (Oroboros). Statistical analysis was performed using Student's *t*-test (* $P < 0.05$; n=4 animals/genotype).

**Figure 3: Oligomycin sensitive respiration (OSR) and mitochondrial maximum respiration capacity (MRC) in human fibroblasts using a Seahorse apparatus**

**A)** OSR analyzed in control and X-ALD fibroblasts cultured in glucose medium or in glucose-free medium containing galactose for 30h, and in the presence or absence of C26:0. **B)** Mitochondrial MRC analyzed in control and X-ALD fibroblasts cultured in glucose medium and in glucose-free medium containing galactose for 30h, in presence or absence of C26:0. Statistical analysis was conducted by ANOVA and Tukey's HSD post hoc (* $P < 0.05$; ** $P < 0.01$; *** $P < 0.001$; n=6/genotype and condition).

**Figure 4: Mitochondria are the main source of ROS induced by excess of C26:0 in human fibroblasts**

**A)** Intracellular (DHE) and mitochondria ROS levels (MitoSOX) measured in X-ALD human fibroblasts after 24h of incubation with C26:0 (20 or 50 μM) or EtOH as vehicle. The complex III inhibitor Antimycin A (500 μM) was used to treat during 4 h as a positive control for mitochondrial ROS production. **B)** ROS levels in control (CTL) and X-ALD human fibroblasts treated with the uncoupling agent CCCP. **C)** ROS levels in CTL and X-ALD human fibroblasts treated with complex V inhibitor oligomycin. **D)** ROS levels in CTL and X-ALD human fibroblasts treated with complex I inhibitor rotenone together with complex II inhibitor TTFA (thenoyltrifluoroacetone). Statistical analysis was conducted by ANOVA and Tukey's HSD post hoc (* $P < 0.05$; ** $P < 0.01$; n=5/genotype and condition).

**Figure 5: Mitochondrial DNA is oxidised in X-ALD patients' fibroblasts and affected white matter brain samples.**

**A)** mtDNA oxidation quantified by Q-PCR in affected and normal-appearing X-ALD white matter. Statistical analysis was performed by ANOVA and Tukey's HSD post hoc (* $P < 0.05$, ** $P < 0.01$; n=9 samples/group). **B)** mtDNA oxidation quantified by Q-PCR in CTL and X-ALD human fibroblasts after an incubation of 24h with C26:0 (20 or 50 μM) or EtOH as vehicle. Statistical analysis was conducted by ANOVA and Tukey's HSD post hoc (* $P < 0.05$; ** $P < 0.01$; n=5/genotype and condition).

**Figure 6: Working model of mitochondrial impairment mediated by excess of C26:0.**

Our proposed model attempts to shed light on the mechanisms of mitochondrial dysfunction in X-ALD, caused by loss of the peroxisomal transporter ABCD1. As hexacosanoic acid (C26:0) cannot enter peroxisomes for degradation, it accumulates intracellularly **(1)**. This excess of C26:0 may affect the inner mitochondrial membrane permeability by unknown mechanisms. As a consequence, this alteration may decrease the $\Delta\Psi m$ **(2)** and generate a certain extent of electron leakage promoting ROS formation **(3)**. These free radicals oxidise mitochondrial proteins of TCA cycle and OXPHOS, leading to impaired bioenergetics and respiration, and also oxidise mtDNA, contributing to a vicious cycle of mitochondrial dysfunction and ultimately, cell demise.

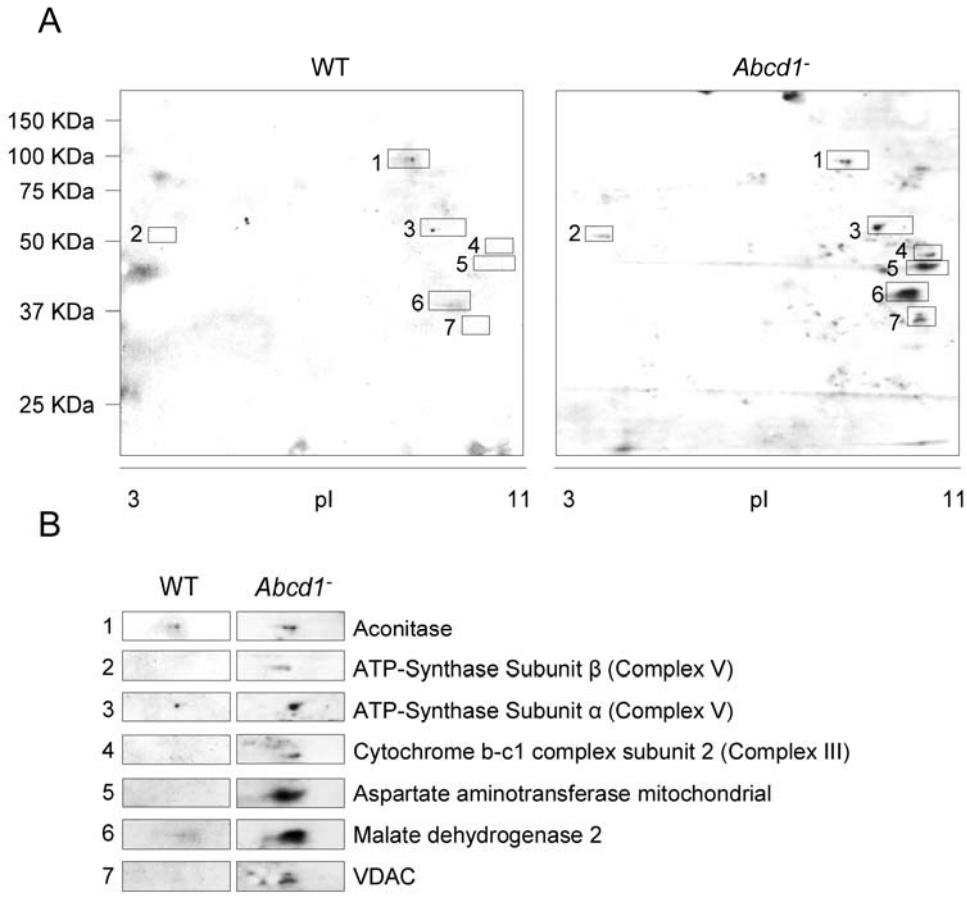
A
WT
Abcd1-
150 KDa
100 KDa
75 KDa
50 KDa
37 KDa
25 KDa
1
2
3
4
5
6
7
3
pI
11
B
WT
Abcd1-
1 Aconitase
2 ATP-Synthase Subunit β (Complex V)
3 ATP-Synthase Subunit α (Complex V)
4 Cytochrome b-c1 complex subunit 2 (Complex III)
5 Aspartate aminotransferase mitochondrial
6 Malate dehydrogenase 2
7 VDAC

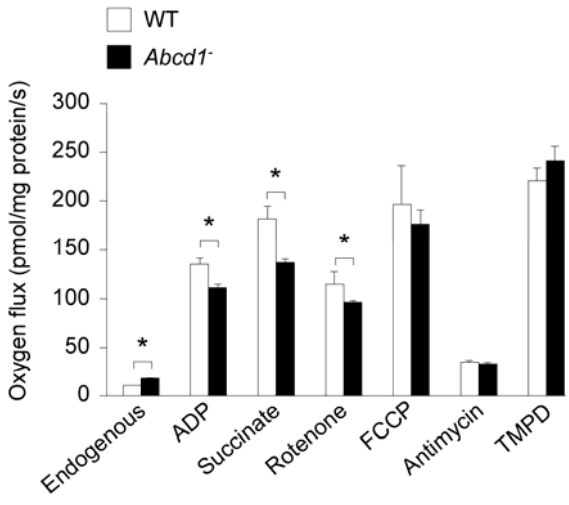
WT
Abcd1-
Oxygen flux (pmol/mg protein/s)
300
250
200
150
100
50
0
*
*
*
*
Endogenous
ADP
Succinate
Rotenone
FCCP
Antimycin
TMPD

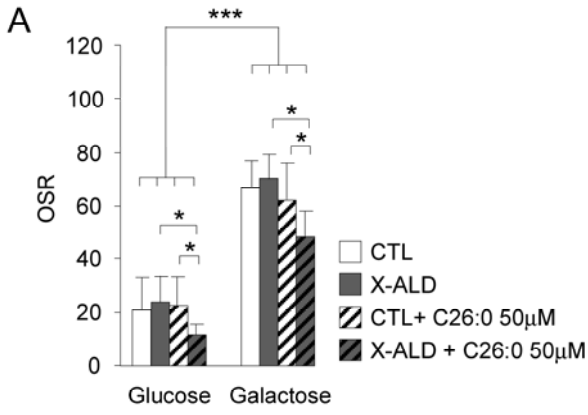
A
***
120
100
80
60
40
20
0
OSR
*
*
*
*
Glucose
Galactose
CTL
X-ALD
CTL+ C26:0 50µM
X-ALD + C26:0 50µM

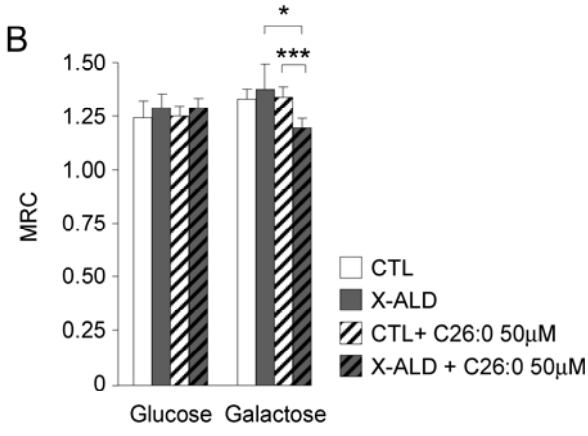
B
*
***
1.50
1.25
1.00
0.75
0.50
0.25
0
MRC
Glucose
Galactose
CTL
X-ALD
CTL+ C26:0 50µM
X-ALD + C26:0 50µM

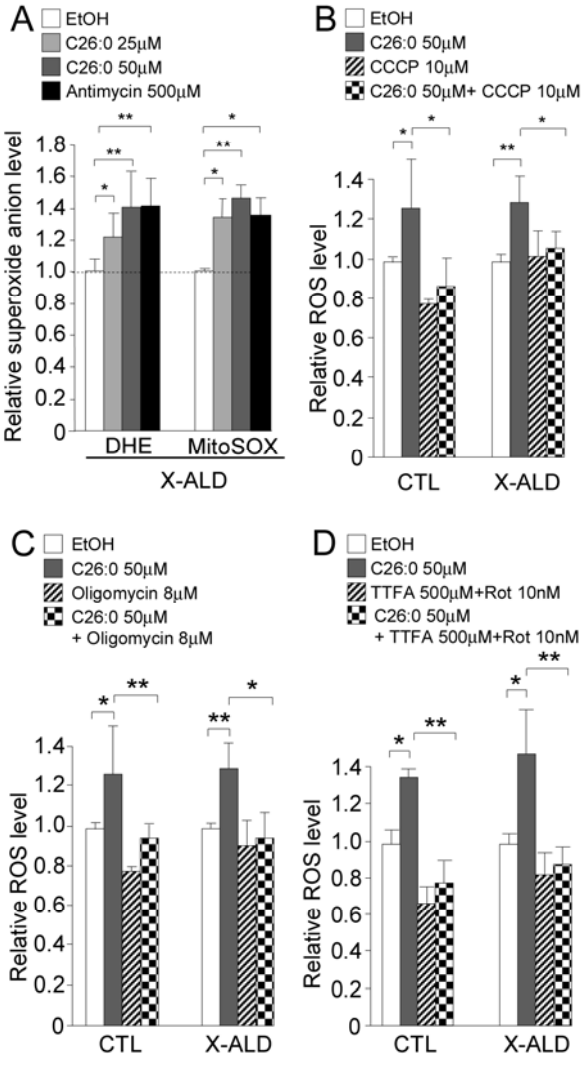
A
EtOH
C26:0 25μM
C26:0 50μM
Antimycin 500μM
Relative superoxide anion level
DHE
MitoSOX
X-ALD
B
EtOH
C26:0 50μM
CCCP 10μM
C26:0 50μM+ CCCP 10μM
Relative ROS level
CTL
X-ALD
C
EtOH
C26:0 50μM
Oligomycin 8μM
C26:0 50μM
+ Oligomycin 8μM
Relative ROS level
CTL
X-ALD
D
EtOH
C26:0 50μM
TTFA 500μM+Rot 10nM
C26:0 50μM
+ TTFA 500μM+Rot 10nM
Relative ROS level
CTL
X-ALD

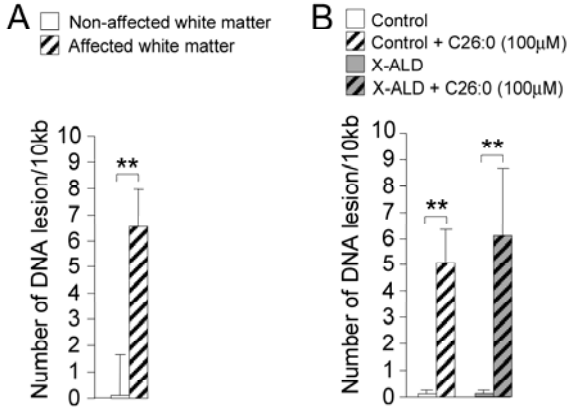
A
Non-affected white matter
Affected white matter
Number of DNA lesion/10kb
0
1
2
3
4
5
6
7
8
9
10
**
B
Control
Control + C26:0 (100μM)
X-ALD
X-ALD + C26:0 (100μM)
Number of DNA lesion/10kb
0
1
2
3
4
5
6
7
8
9
10
**
**

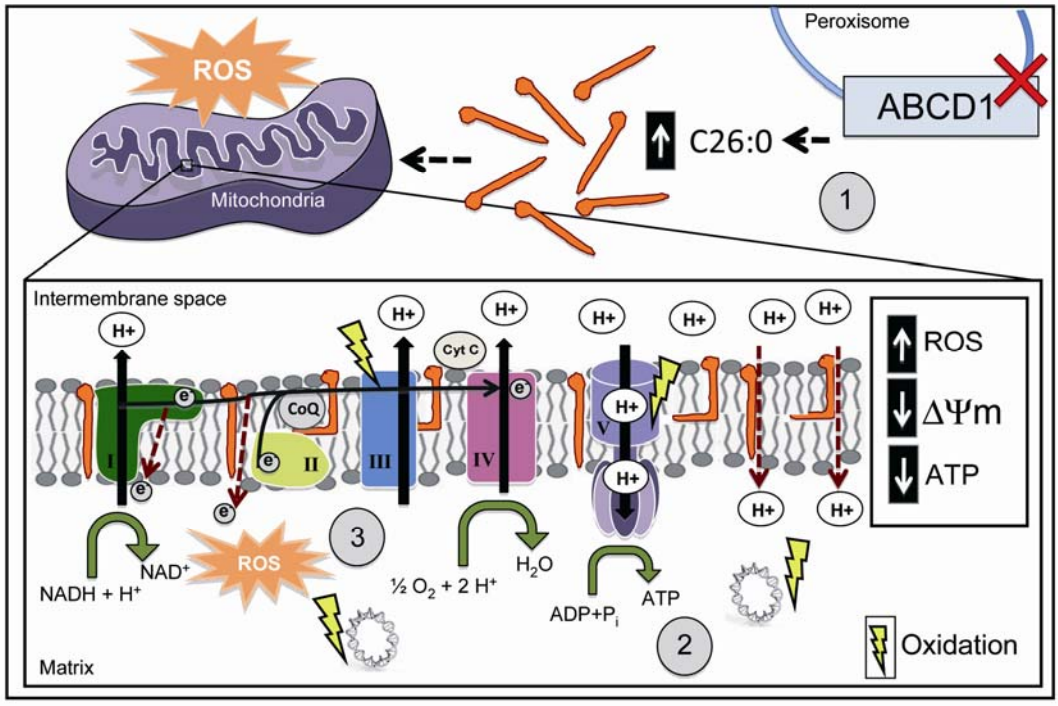
Peroxisome
ROS
ABCD1
C26:0
Mitochondria
1
Intermembrane space
H+
Cyt C
CoQ
I
II
III
IV
V
ROS
ΔΨm
ATP
NADH + H+
NAD+
ROS
3
½ O2 + 2 H+
H2O
ADP+Pi
ATP
2
Matrix
Oxidation